Tian, J.; Chen, S.; Masoller, C. (2017) Generation of extreme pulses on demand in semiconductor lasers with optical injection. *Optics express*. Vol. 25, issue 25, p. 31326- 31336. DOI: 10.1364/OE.25.031326

Research Article | Vol. 25, No. 25 | 11 Dec 2017 | OPTICS EXPRESS 31326
Optics EXPRESS

Generation of extreme pulses on demand in semiconductor lasers with optical injection

TIAN JIN,[1,3] CHEN SIYU,[2,3] AND CRISTINA MASOLLER[3,*]

[1]School of Opto-Electronics, Beijing Institute of Technology, Beijing, 100081, China
[2]State Key Laboratory of Precision Measurement Technology and Instruments, Department of Precision Instrument, Tsinghua University, Beijing 100084, China
[3]Departament de Fisica, Universitat Politecnica de Catalunya, Colom 11, 08222 Terrassa, Barcelona, Spain
[*]cristina.masoller@upc.edu

Abstract: The generation of extreme intensity pulses in an optically injected semiconductor laser is studied numerically by using a well-known rate equation model. We show that step-up perturbations of the laser pump current can trigger extreme pulses. We study the perturbation parameters (amplitude, duration) that are more likely to trigger a extreme pulse, and compare the properties of the generated extreme pulses with those spontaneous emitted, which are due to the intrinsic deterministic dynamics of the laser. We study how the phase of the optical field evolves during the pulses and compare both types of pulses (generated by external perturbations and generated by intrinsic nonlinear dynamics). We find that in both cases the phase dynamics is similar with an abrupt rise and fall: as an extreme pulse begins, the phase grows abruptly and reaches a local maximum at the peak of the pulse, then, when the pulse is over, the phase falls down to a value which is similar to the one before the pulse started.

OCIS codes: (140.1540) Chaos; (140.5960) Semiconductor lasers; (250.5960) Semiconductor lasers.

References and links

1. D. R. Solli, C. Ropers, P. Koonath, and B. Jalali, "Optical rogue waves," Nature **450**, 1054–1057 (2007).
2. A. N. Pisarchik, R. Jaimes-Reategui, R. Sevilla-Escoboza, G. Huerta-Cuellar, and M. Taki, "Rogue waves in a multistable system," Phys. Rev. Lett. **107**, 274101 (2011).
3. M. G. Kovalsky, A. A. Hnilo, and J. R. Tredicce, "Extreme events in the Ti:sapphire laser," Opt. Lett. **36**, 4449–4451 (2011).
4. K. Schires, A. Hurtado, I.D. Henning, and M.J. Adams, "Rare disruptive events in the polarisation-resolved dynamics of optically-injected 1550nm-VCSELs," Electron. Lett. **48**, 872–874 (2012).
5. C. Lecaplain, Ph. Grelu, J. M. Soto-Crespo, and N. Akhmediev, "Dissipative rogue waves generated by chaotic pulse bunching in a mode-locked laser," Phys. Rev. Lett. **108**, 233901 (2012).
6. A. Karsaklian Dal Bosco, D. Wolfersberger, and M. Sciamanna, "Extreme events in time-delayed nonlinear optics," Opt. Lett. **38**, 703–705 (2013).
7. C. Metayer, A. Serres, E. J. Rosero, W. A. S. Barbosa, F. M. de Aguiar, J. R. Rios Leite, and J. R. Tredicce, "Extreme events in chaotic lasers with modulated parameter," Opt. Express **22**, 19850 (2014).
8. M. W. Lee, F. Baladi, J. R. Burie, M. A. Bettiati, A. Boudrioua, and A. P. A. Fischer , "Demonstration of optical rogue waves using a laser diode emitting at 980 nm and a fiber Bragg grating," Opt. Lett. **41**, 4476 (2016).
9. N. Akhmediev, B. Kibler, F. Baronio, et al., "Roadmap on optical rogue waves and extreme events," J. Opt. **18**, 063001 (2016).
10. N. Akhmediev, A. Ankiewicz, and M. Taki, "Waves that appear from nowhere and disappear without a trace," Phys. Lett. A **373**, 675 (2009).
11. C. Kharif, E. Pelinovsky, and A. Slunyaev, *Rogue Waves in the Ocean* (Springer, 2009).
12. C. Bonatto, M. Feyereisen, S. Barland, M. Giudici, C. Masoller, J. R. Rios Leite, and J. R. Tredicce, "Deterministic optical rogue waves," Phys. Rev. Lett. **107**, 053901 (2011).
13. J. Zamora-Munt, B. Garbin, S. Barland, M. Giudici, J. R. Rios Leite, C. Masoller, and J. R. Tredicce, "Rogue waves in optically injected lasers: origin, predictability, and suppression," Phys. Rev. A. **87**, 035802 (2013).
14. S. Wieczorek, B. Krauskopf, T.B. Simpson, and D. Lenstra, "The dynamical complexity of optically injected semiconductor lasers," Phys. Rep. **416**, 1–128 (2005).
15. D. O'Shea, S. Osborne, N. Blackbeard, D. Goulding, B. Kelleher, and A. Amann, "Experimental classification of dynamical regimes in optically injected lasers," Opt. Express **22**, 21701 (2014).
16. M. Sciamanna and K. A. Shore, "Physics and applications of laser diode chaos," Nat. Phot. **9**, 151 (2015).

#307422 https://doi.org/10.1364/OE.25.031326
Journal © 2017 Received 19 Sep 2017; revised 19 Nov 2017; accepted 23 Nov 2017; published 1 Dec 2017

Optics EXPRESS

17. R. Karnatak, G. Ansmann, U. Feudel, and K. Lehnertz, "Route to extreme events in excitable systems," Phys. Rev. E **90**, 022917 (2014).
18. A Saha and U. Feudel, "Extreme events in FitzHugh-Nagumo oscillators coupled with two time delays", Phys. Rev. E **95**, 062219 (2017).
19. C. Bonazzola, A. Hnilo, M. Kovalsky, and J. R. Tredicce, "Optical rogue waves in an all-solid state laser with saturable absorber: importance of spatial effects," J. Opt. **15**, 064004 (2013).
20. C. Rimoldi, S. Barland, F. Prati, and G. Tissoni, "Spatiotemporal extreme events in a laser with a saturable absorber," Phys. Rev. A **95**, 023841 (2017).
21. S. Coulibaly, M. G. Clerc, F. Selmi, and S. Barbay, "Extreme events following bifurcation to spatiotemporal chaos in a spatially extended microcavity laser," Phys. Rev. A **95**, 023816 (2017).
22. N. Akhmediev, J. M. Soto-Crespo, and A. Ankiewicz, "How to excite a rogue wave," Phys. Rev. A **80**, 043818 (2009).
23. D. Pierangeli, G. Musarra, F. Di Mei, G. Di Domenico, A. J. Agranat, C. Conti, and E. DelRe, "Enhancing optical extreme events through input wave disorder," Phys. Rev. A **94**, 063833 (2016).
24. M. Turconi, B. Garbin, M. Feyereisen, M. Giudici, and S. Barland, "Control of excitable pulses in an injection-locked semiconductor laser," Phys. Rev. E **88**, 022923 (2013).
25. B. Garbin, A. Dolcemascolo, F. Prati, J. Javaloyes, G. Tissoni, and S. Barland, "Refractory period of an excitable semiconductor laser with optical injection," Phys. Rev. E **95**, 012214 (2017).
26. A. Hurtado and J. Javaloyes, "Controllable spiking patterns in long-wavelength vertical cavity surface emitting lasers for neuromorphic photonics systems," Appl. Phys. Lett. **107**, 241103 (2015).
27. J. Robertson, T. Deng, J. Javaloyes and A. Hurtado, "Controlled inhibition of spiking dynamics in VCSELs for neuromorphic photonics: theory and experiments," Opt. Lett. **42**, 1560–1563 (2017).
28. S. Perrone, R. Vilaseca, J. Zamora-Munt, and C. Masoller, "Controlling the likelihood of rogue waves in an optically injected semiconductor laser via direct current modulation," Phys. Rev. A **89**, 033804 (2014).
29. J. Ahuja, D. Bhiku Nalawade, J. Zamora-Munt, R. Vilaseca and C. Masoller, "Rogue waves in injected semiconductor lasers with current modulation: role of the modulation phase," Opt. Express **22**, 28377 (2014).
30. B. Kelleher, D. Goulding, B. Baselga Pascual, S.P. Hegarty, and G. Huyet, "Phasor plots in optical injection experiments," Eur. Phys. J. D **58**, 175 (2010).
31. B. Kelleher, D. Goulding, B. Baselga Pascual, S. P. Hegarty, and G. Huyet, "Bounded phase phenomena in the optically injected laser," Phys. Rev. E **85**, 046212 (2012).

1. Introduction

Laser systems displaying extreme optical pulses, often referred to as optical rogue waves (RWs) [1], are being intensively investigated as they are excellent test beds to study extreme fluctuations under controlled conditions [2–9]. Rogue waves have been observed in many systems and were initially found in hydrodynamics, where occasionally, huge waves in ocean waters have been reported that, in contrast to tsunamis or solitons, can appear from nowhere, disappear in a short spatial length and do not necessarily propagate for long distances [10].

Optical RWs are ultra–high intensity pulses that are qualitatively characterized by a long-tail in the probability distribution function (pdf) of intensity values. Quantitatively, the precise definition of an extreme pulse depends on the system under investigation. A RW is often defined in terms of the abnormality index, which is the ratio between the height of the wave and the average wave height among one-third of the highest waves, and every wave whose abnormality index is larger than 2 is considered a RW [11]. An alternative approach to define RWs is to use a threshold, τ, that is defined as the mean value, $\langle S \rangle$, and several (6-8) standard deviations, σ, of the distribution of intensity values.

A technologically relevant example of a laser system displaying ultra-high pulses is a continuous-wave (cw) optically injected semiconductor laser [12, 13]. It displays a rich variety of dynamical regimes [14, 15], including injection locking, periodic oscillations and chaotic behavior, which have found various applications [16]. As shown in [12], optical rogue waves appear in regions of the parameter space where the dynamics is chaotic. However, chaos is not enough to observe RWs as there are regions of chaotic dynamics with RWs and others without RWs. It is therefore important to understand which are the physical mechanisms that are ultimately responsible for generating extreme fluctuations [17, 18].

In the case of injected semiconductor lasers it has been shown, by using the simplest rate-equation model, that a small region of the phase space can lead to a RW when it is visited by the

Optics EXPRESS

trajectory [13]. In the chaotic regions with RWs, the trajectory can access a narrow region of the phase space (referred to as "the rogue wave door") where the stable one-dimensional manifold of a saddle point (referred to as S2) is located. Whenever the trajectory closely approaches this region, a RW is likely to occur. The mechanism is as follows: the trajectory evolves along the stable manifold towards S2, which is the solution with high carrier density and low intensity. However, S2 has a two-dimensional unstable manifold, and thus, the trajectory also spirals out. During the evolution along the stable manifold of S2 the system accumulates carriers while it approaches a low intensity, and therefore, a high pulse is emitted. The duration of the evolution along the stable manifold of S2 is irregular because it varies with the initial "entry" conditions and is affected by numerical noise, and in consequence, there is a wide distribution of pulse heights. In contrast, in the chaotic regions without RWs, the trajectory never approaches the dangerous region of the phase space where the "RW door" (the one-dimensional stable manifold of S2) is located. In [13] it was also shown that RWs occur when an abrupt expansion of the attractor enables access to that particular region of phase space.

Optical rogue waves have also been investigated in laser models that include spatial degrees of freedom (one or two dimensions) [9]. While in these models extreme pulses might still be generated by a similar mechanism as in the rate-equation model (the presence of a narrow-channel or a "RW door" in the phase space), due to the high-dimensionality of the phase space this special region is difficult to identify. In addition, in the presence of spatial degrees of freedom, several other features can be relevant for understanding the RW phenomenon [9, 19–21].

While previous work has shown that special initial conditions [22] or input wave disorder [23] can facilitate the excitation of rogue waves, a relevant open question that has not yet been addressed is the following: is it possible to generate extreme optical pulses "on demand"?. More specifically, in parameter regions without RWs, is it possible to perturb the system in such a way that the trajectory approaches the "RW door", and therefore, an extreme pulse is likely to be triggered? The generation on demand of ultra high-intensity light pulses could find applications for imaging and for sensing. For example, short laser pulses are routinely used to visualize the biological world, and the controlled generation of pulses with ultra-high peak temporal intensity can reduce the signal-to-noise ratio, thus increasing the image quality. For sensing, a small variation of a control parameter (here we focus on a small perturbation of the laser current) can be easily detected because it generates a light pulse with high peak intensity.

In an optically injected semiconductor laser the effects of periodic perturbations of the phase of the injected field have been studied experimentally in Refs. [24, 25]. In the injection locking region (where the laser emits a stable output) it was shown that excitable light pulses could be triggered, if the perturbation was strong enough. In addition, recent works have reported the controllable generation and suppression of optical pulses via perturbations encoded in the amplitude of the injected signal [26, 27]. Here we consider a different situation: we analyze a parameter region outside the injection-locking region (i.e., the laser output displays small periodic or chaotic oscillations), and try to generate high intensity pulses by applying perturbations to the laser pump current, at random times. By extensive model simulations we demonstrate that step-up perturbations of the pump current parameter can trigger extreme pulses, with a success rate that depends on various parameters. We analyze the dynamics of the phase of the optical field during the pulses and find that in both cases (pulses generated by an external perturbation and generated by intrinsic nonlinear dynamics) the phase dynamics consists of an abrupt rise and fall, reaching a local maximum at the peak of the pulse.

Optics EXPRESS

2. Model

The rate equations describing the dynamics of a continuous-wave (cw) optically injected semiconductor laser are [12, 13]:

$$\frac{dE}{dt} = \kappa(1+i\alpha)(N-1)E + i\Delta\omega E + \sqrt{P_{inj}} \quad (1)$$

$$\frac{dN}{dt} = \gamma_N(\mu(t) - N - |E|^2) \quad (2)$$

where E is the slow envelope of the complex optical field, $S = |E|^2$ is the intensity, N is the carrier density, κ is the field decay rate, α is the line-width enhancement factor, and γ_N is the carrier decay rate. $\Delta\nu = \Delta\omega/2\pi$ with $\Delta\omega = \omega_s - \omega_m$ is the frequency detuning between the injected and the master laser and P_{inj} is the injection strength. $\mu(t)$ is the injection current parameter (normalized such that the threshold of the free-running laser is at μ_{th}=1), to which a step-up perturbation of amplitude $\Delta\mu$ and duration τ is applied at random times, as shown in Fig. 1.

In this model, in parameter regions where the intensity dynamics only displays small oscillations, the inclusion of spontaneous emission noise can lead to the generation of rare and extreme pulses [13, 28]. Therefore, we simulate the deterministic model because we are interested in quantifying the likelihood of generating extreme pulses by pump current perturbations, and the inclusion of noise in the simulations would hinder the interpretation of the results, because a pulse following a perturbation could have been triggered by the perturbation, or it could have been triggered by noise.

3. Results

The model equations were numerically solved using the same parameters as in [12, 13]: $\kappa = 300$ ns^{-1}, $\alpha = 3$, $\gamma_N = 1$ ns^{-1}, $P_{inj} = 60$ ns^{-2}, and the other parameters are indicated in the figure captions. The relation between the model parameters and the experimental parameters is discussed in detail in [14]. Here we use this set of parameters because in [12, 13] the simulations were found to be in qualitative good agreement with the experimental observations. To provide an estimate of the pump current and optical injection power, we remark that in both works a VCSEL was used with pump current about 1 mA and injected power 1.1 mW ([12]) and pump current about 0.4 mA and injected power 21 μW ([13]).

As discussed in the Introduction, in this model ultra-high intensity pulses, that have been referred to as deterministic RWs [12], occur in specific parameter regions (see Figs. 1 and 3 in [12], Figs. 4 and Fig. 5a in [13] and Fig. 1 in [28]). A typical intensity time series displaying sporadic extreme pulses is shown in Fig. 1 left. For parameters such that the intensity displays only small oscillations, extreme pulses can be induced by a step-up perturbation of the pump current parameter, and an example of a generated RW is displayed in Fig. 1 right. We have also analyzed the effect of step-down current perturbations and found that they did not trigger extreme pulses. We speculate that this is due to the fact that the "RW door" is the stable 1D manifold of the saddle point S2 which has high carrier density and low intensity [13], and because a step down perturbation of the pump current abruptly decreases the carrier density, it prevents the trajectory to approach the vicinity of S2 (in other words, an extreme pulse can be emitted when N is high, and a step-down current perturbation diminishes the carrier population).

We will focus the study in the parameter regions where there are no spontaneous ultra-high pulses, and will present results for two sets of parameters, labeled B ($\mu = 2.2$ and $\Delta\nu = 0.6$ GHz) and C ($\mu = 1.8$ and $\Delta\nu = 0.22$ GHz), which are located close to the boundary of the RW region (see Fig. 1 in [28]). The pulses generated by external perturbations will be compared with spontaneous pulses, and for the comparison we will consider a third set of parameters, labeled A ($\mu = 2.4$ and $\Delta\nu = 0.22$ GHz), where there are spontaneous pulses (shown in Fig. 1).

Optics EXPRESS

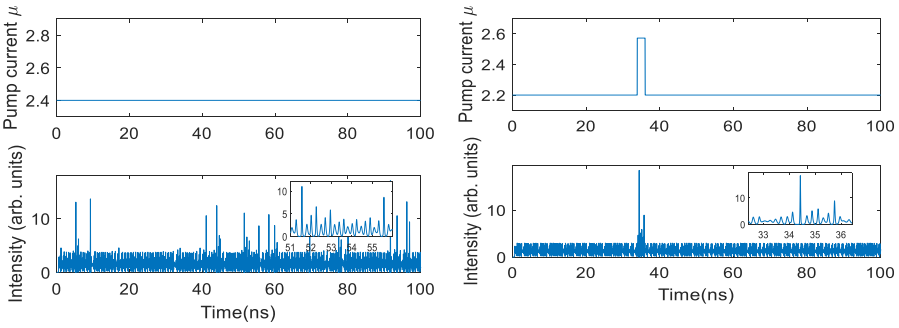

Fig. 1. Left: Intensity temporal evolution (bottom line) at constant pump current (top line): the intensity displays small oscillations but, occasionally, very high pulses are generated by deterministic nonlinear dynamics. The parameters are $\mu = 2.4$ and $\Delta\nu = 0.22$ GHz (point labeled A). Right: Example of pump current step-up perturbation (top line) and the generated pulse (bottom line). The parameters are $\mu = 2.2$ and $\Delta\nu = 0.6$ GHz (point labeled B). The insets show the details of the pulses.

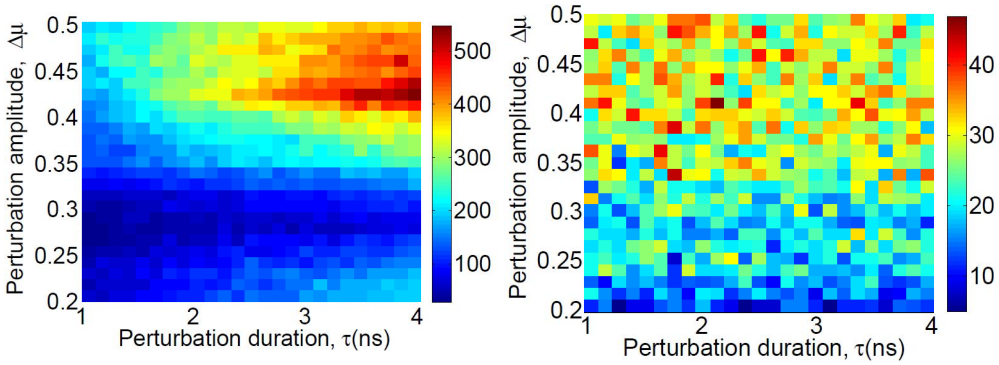

Fig. 2. Number of intensity pulses generated after 1000 perturbations as a function of the perturbation parameters. In point C (left) the success probability can exceed 50%, while in point B (right) it is much lower.

To quantify the effectiveness of a perturbation of the pump current we generated 1000 trajectories of 120 ns each (starting from random initial conditions), and we randomly selected the perturbation moment in the interval of 10 ns to 100 ns. Then, we counted how many times an extreme pulse was generated, using $\langle S \rangle + 8\sigma$ as threshold to define a extreme pulse. Then, we varied the perturbation parameters (amplitude, $\Delta\mu$, and duration, τ) to determine if there are optimal values of $(\Delta\mu, \tau)$ that result in a larger number of pulses. The results are presented in Fig. 2 that displays the number of pulses in the plane $(\Delta\mu, \tau)$ when the laser parameters are points C and B. We can observe that the success of the perturbation is different, while in point C (left panel) some perturbations have more than 50% probability of triggering a high pulse, in point B (right panel) it is much lower. In Fig. 2 we also note that, if the perturbation amplitude is large enough, as the duration τ increases (while $\Delta\mu$ is kept constant) there is a gradual increase in the number of extreme pulses generated. This indicates that extreme pulses are less likely to be triggered by short perturbations. Figure 3 shows the response to two perturbations with the same amplitude: one triggers an extreme pulse, while the other only produces a small fluctuation. We speculate that the effect of the duration of the perturbation is related to the increase of the carrier density: if the pump current is $\mu + \Delta\mu$ during a long enough time interval, it will likely increase

Optics EXPRESS

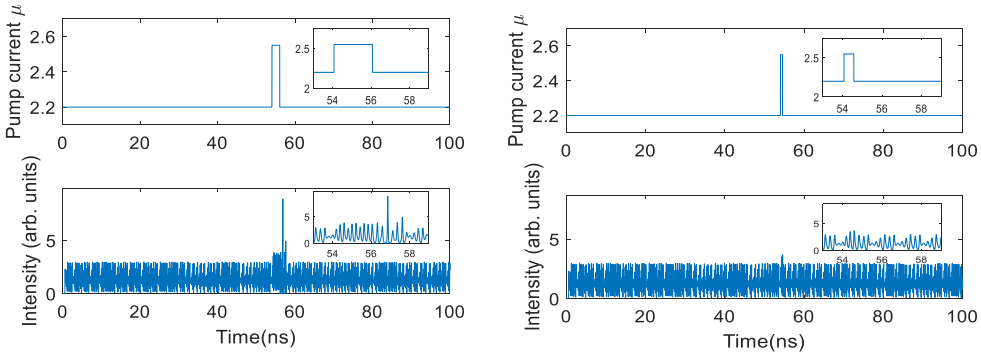

Fig. 3. Examples of two current perturbations: one triggers an extreme pulse while the other only produces a small fluctuation. The parameters are $\mu = 2.2$, $\delta\nu = 0.6$ GHz, $\Delta\mu = 0.35$, and $\tau = 2$ ns (left), 0.5 ns (right).

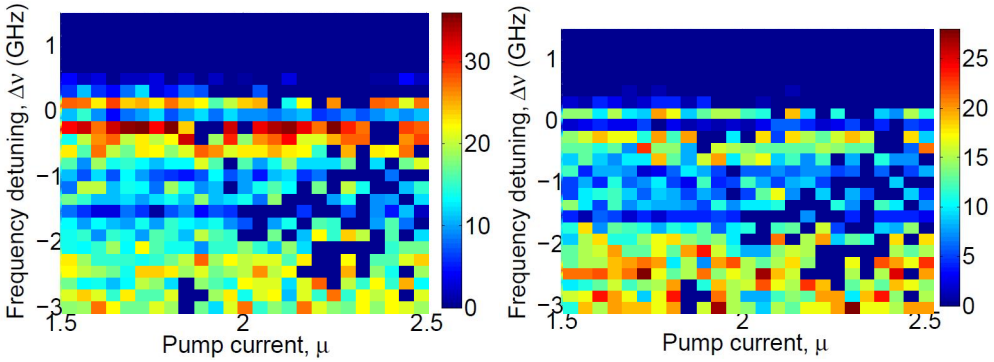

Fig. 4. Number of generated intensity pulses as a function of the pump current, μ, and the frequency detuning, $\Delta\nu$. 100 perturbations are performed with parameters $\Delta\mu = 0.35$ and $\tau = 4$ (left) and $\Delta\mu = 0.35$ and $\tau = 2$ (right). In the regions where there are spontaneous extreme pulses, no perturbation is applied and thus the number of generated pulses is zero.

the carrier density enough to approach the vicinity of the "RW door" (the stable 1D manifold of the saddle point S2 that has high N and small $|E|$).

To analyze which are the laser operation conditions for which the perturbation is more likely to be effective we kept $(\Delta\mu, \tau)$ fixed and varied the laser parameters (pump current, μ, frequency detuning, $\Delta\nu$). The plot of the number of generated high pulses, displayed in Fig. 4, reveals that pulses can be triggered in large parameter regions, with widely different success rates. For example, for $\Delta\mu = 0.35$, $\tau = 3$ ns, in point C 200 perturbations resulted in 47 pulses, while in point B, 1500 perturbations were required to trigger a similar number of pulses.

To analyze if the generated intensity pulses are somehow different from spontaneous high pulses, we analyzed the evolution of the phase of the optical field during the pulses.

We first consider point A, where spontaneous high pulses occur, and simulated 50 intensity time traces of 200 ns. Figure 5 displays the pulses above $\langle S\rangle + 8\sigma$, centered at the maximum of rogue wave. The phase time trace is also displayed, with the value of the phase at the peak of the rogue wave subtracted to make all the phase trajectories converge to zero at the time when the intensity is maximum. It can be observed that, as the extreme pulse begins, the phase grows abruptly and reaches a local maximum at the peak of the pulse, then, when it is over, the

Optics EXPRESS

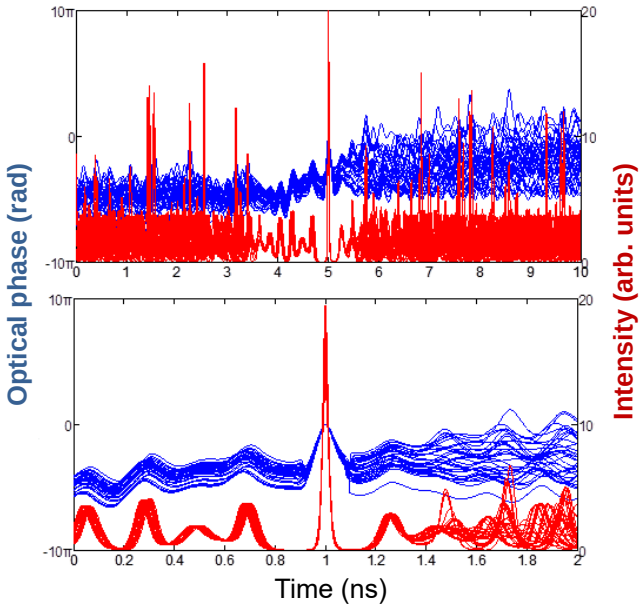

Fig. 5. Intensity and phase time traces during pulses that are generated by the intrinsic nonlinear dynamics. The lower panel shows in detail the temporal evolution during the pulse. 50 intensity time traces of 200 ns each were simulated and 816 pulses were above the $\langle S \rangle + 8\sigma$ threshold. The intensity time traces are superposed and centered at the peak of the pulse. The phase time traces are also superposed and the value of the phase at the pulse peak is subtracted to make all time traces converge to zero at the peak. The lower panels show in detail the evolution during the intensity peak. Parameters correspond to point A.

phase falls down to a similar value as before the pulse started. To demonstrate the robustness of this observation, we also performed simulations including a sinusoidal modulation in the pump current. The results are presented in Fig. 6. As expected [28, 29], the number of pulses decreases significantly (without current modulation there are 816 extreme pulses, while with modulation, only 78); however, the phase dynamics is the same. The corresponding evolution of the carrier density is shown in Fig. 7 , where we observe that before the pulse N increases linearly, when the pulse is emitted N decreases abruptly, and then N recovers again linearly. The linear increase before the pulse is due to the fact that the trajectory, before the pulse, moves along the stable 1D manifold, towards the saddle fixed point S2 that has high N and low $|E|$ values [13]. A qualitatively similar dynamics is seen in Figs. 8 and 9, where now the pulses are generated by perturbations of the pump current parameter.

Next, we discuss the statistics of the generated pulses in terms of their mean amplitude and mean waiting time (i.e., the time between the start of the perturbation and the peak of the pulse). Figure 10 shows that the highest amplitudes are obtained near parameter regions where spontaneous extreme pulses are generated, and typically, if the perturbation is successful, the average waiting time before the pulse is emitted is about 1-2 ns. However, the distribution of waiting time is in general bi-modal: extremely high pulses are typically emitted shortly after the perturbation starts (the waiting time is about 0.5 ns) while pulses that are above the threshold but not too extreme can be emitted after a longer time (typically 2-5 ns).

We conclude by discussing the role of shape of the step-up perturbation. As it is experimentally impossible that the pump current changes from μ to $\Delta\mu$ instantaneously, it is important to investigate if extreme pulses can also be generated when the current perturbations are smooth.

Optics EXPRESS

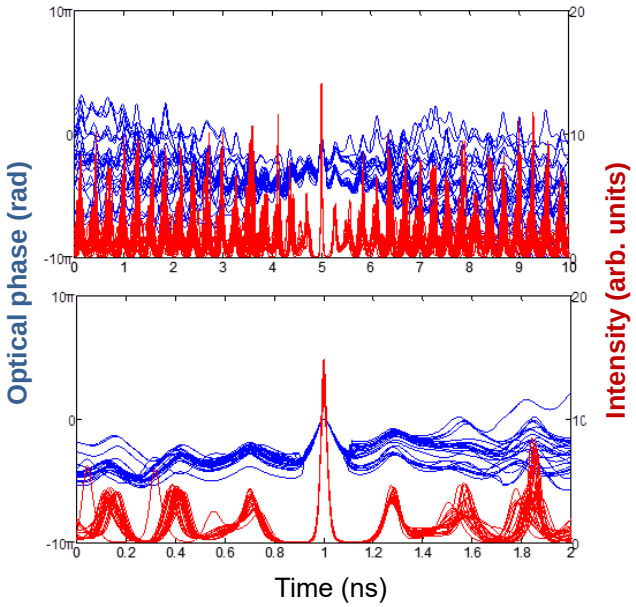

Fig. 6. As Fig. 5 but the pump current parameter is sinusoidally modulated, $\mu = \mu_0[1 + A_{mod}\sin(2\pi f_{mod}t)]$ with $\mu_0 = 2.4$, $A_{mod} = 0.2$ and $f_{mod} = 3.5$ GHz. In 50 time traces of 200 ns each there were 78 pulses higher than $\langle S\rangle + 8\sigma$.

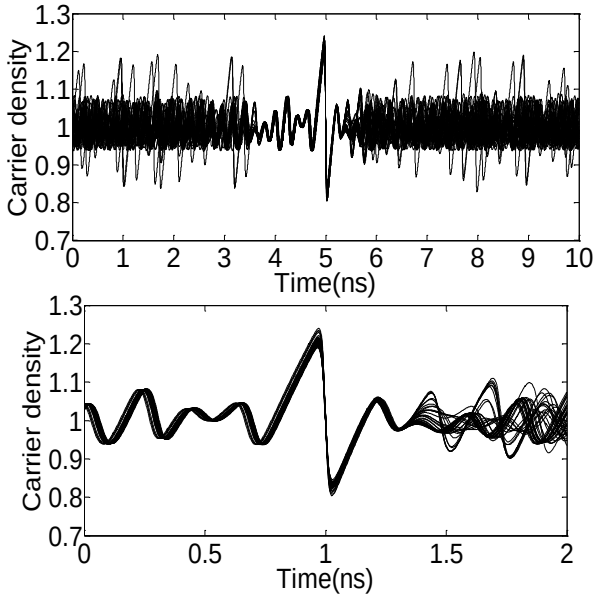

Fig. 7. Temporal evolution of the carrier density during the spontaneous extreme pulses shown in Fig. 5.

Optics EXPRESS

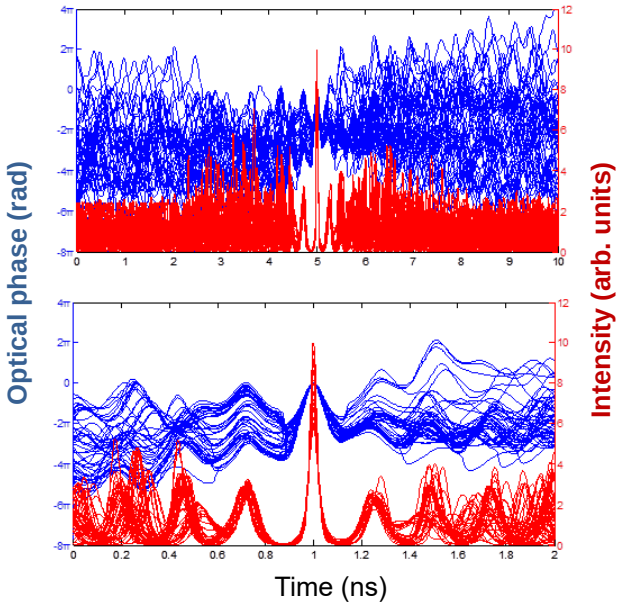

Fig. 8. Intensity and phase time traces during pulses generated by pump current perturbations. The lower panel shows in detail the temporal evolution during the pulses. 200 simulations were done and in each simulation a perturbation ($\Delta\mu = 0.35$ and $\tau = 3$ ns) was randomly applied to the laser current. The resulting 47 pulses above the threshold ($\langle S\rangle + 8\sigma$) are superposed and centered at the peak of the pulse. As in Figs. 5 and 6 the phase time traces are also superposed and the value of the phase at the peak of the pulse is subtracted to make all time traces converge to zero at the pulse peak. Parameters are $\mu = 1.8$, $\Delta\nu = 0.22$ GHz (point C).

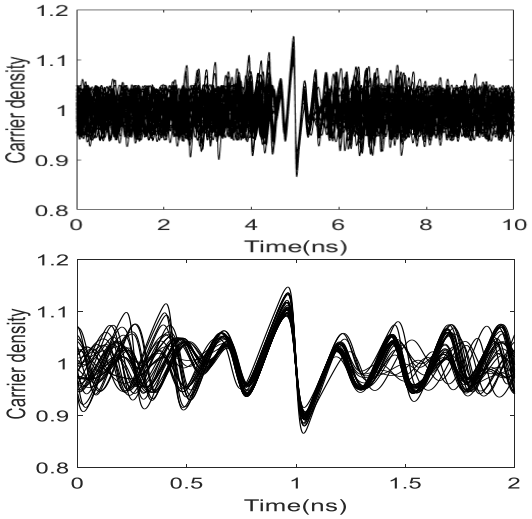

Fig. 9. Temporal evolution of the carrier density during the extreme pulses that are generated by step-up current perturbations.

Optics EXPRESS

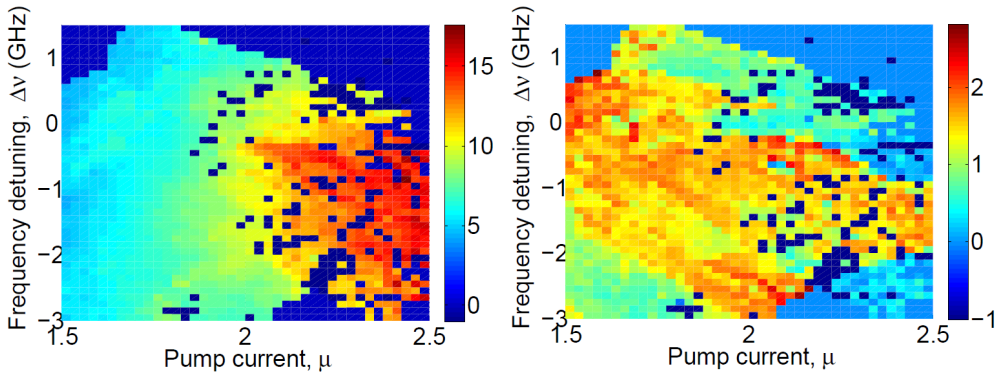

Fig. 10. Mean amplitude (left panel, in arb. units) and mean waiting time (right panel, in nanoseconds) of the pulses generated by current perturbation with parameters $\Delta\mu = 0.35$ and $\tau = 3$ ns. Regions where spontaneous ultra-high pulses occur are indicated in dark blue.

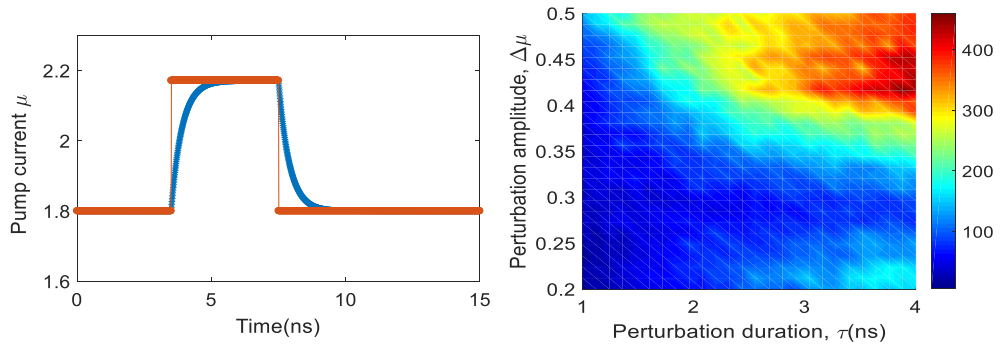

Fig. 11. Left: abrupt and smooth pump current perturbation; right: number of extreme pulses generated by smooth perturbations, when the parameters are as in Fig. 2, right panel.

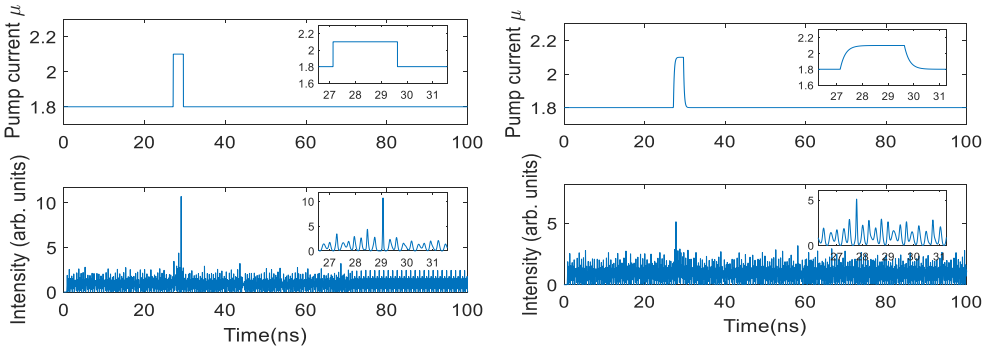

Fig. 12. Abrupt (left) and smooth (right) pump current perturbation and the resulting intensity pulses. It can be noticed that the height of the pulse generated by the smooth perturbation is lower than that the height of the pulse generated by the abrupt perturbation.

Optics EXPRESS

Intuitively, if the perturbation is smooth enough, the system can be able to follow the perturbation and an extreme pulse might not be triggered, or the system might emit a pulse whose peak amplitude is smaller, with respect to the pulse triggered by a sharp current perturbation. Our simulations indicate that this is indeed the case: as seen in Fig. 11 the number of generated pulses is smaller and, as an example, Fig. 12 presents the comparison of two pulses that are generated by a sharp and by a smooth perturbation; here we can see that the pulse generated by the smooth perturbation has lower amplitude.

4. Conclusion

To summarize, we have simulated the dynamics of an optically injected semiconductor laser with parameters close to the boundary of the region where extreme pulses are occasionally spontaneously generated by the intrinsic nonlinear dynamics of the system, to investigate the possibility of generating them "on demand" by means of an external pump current perturbation. We found that, for appropriated parameters, a step-up perturbation of the laser current can have more than 50% probability of generating an extreme pulse. The success probability depends on the laser parameters and on the perturbation parameters.

We have also compared the "spontaneous" and the perturbation–generated extreme pulses, and in order to try to identify possible differences, we analyzed the dynamics of the phase during the intensity pulses. While a phase-intensity relationship can be expected due to the α-factor, such relation is not trivial as the phase depends on both, the field amplitude, $|E|$, and the carrier density, N [14]. We have found that during both types of extreme pulses, the dynamics of the phase is remarkable similar, which suggests that also when the pulses are generated by a current perturbation, the trajectory approaches the "Rogue Wave door" [13], i.e., moves along and follows the stable 1D manifold of the saddle fixed point that has high N and low $|E|$ values.

While we have investigated the role of the pump current, the detuning, the amplitude of the perturbation and the duration of the perturbation, several other model parameters can play an important role in enhancing or inhibiting the generation "on demand" of extreme pulses (for example, the injected power, the noise strength and the alpha-factor). The role of these parameters deserve a detailed investigation, which is outside the scope of the present work and is left for future work (here we limit the study to a set of "familiar" parameters which are known to provide a good qualitative agreement with experiments [12, 13]). We cannot exclude the existence of optimal parameters that give a very high (maybe up to 100%) probability of generating an extreme pulse, however, we have not found them (our best probability is up to 50%). We speculate that the pump current perturbation needs to produce a very precise effect: the carrier density needs to reach a high enough value while the intensity needs to be low enough; otherwise, a high pulse is not emitted. The large number of parameters leaves open the possibility of finding other sets of parameters that can be more optimal for generating extreme pulses.

We hope that our numerical results will motivate experimental studies on the possibility of triggering ultra-high pulses by small perturbations. In addition, as the optical phase can be resolved experimentally by using the technique demonstrated in Refs. [30, 31], we hope that our work will motivate experimental studies of the phase dynamics during extreme pulses. It would also be interesting to explore the applicability of this method to other laser systems.

Funding

Spanish MINECO/FEDER (FIS2015-66503-C3-2-P); ICREA ACADEMIA, Generalitat de Catalunya.

Acknowledgments

T. J. and C. S. contributed equally to this work.